*Technical Physics Letters, 2022, Vol. 48, No. 6*

*01.5;09.5*

# A multi−frequency synchronous self−oscillations in fiber lasers with optomechanical microoscillators

© *F.A. Egorov*

Fryazino Branch, Kotel'nikov Institute of Radio Engineering and Electronics, Russian Academy of Sciences, Fryazino, Moscow oblast, Russia
E-mail: egorov-fedor@mail.ru

*Received March 28, 2022*
*Revised April 29, 2022*
*Accepted May 1, 2022*

In erbium−ytterbium fiber lasers with mirrors based on sets of optomechanical microoscillators, modes of multi−frequency (up to five frequencies) synchronous self−oscillations are implemented. Microoscillators are made in the form of a silicon microbeams array with a quasi−equidistant spectrum of elastic vibration modes excited by laser radiation pressure. A significant dependence of self−oscillations on the spectral properties of optical resonator mirrors has been revealed, which is explained within the framework of the concepts of inhomogeneous broadening in the active fiber.

**Keywords:** fiber lasers, self−oscillations, optomechanical microoscillators.

DOI: 10.21883/TPL.2022.06.53791.19203

In Fabry−Perot resonators with optomechanical microoscillators (OMO) used as mirrors, the OMO elastic deformations (oscillations) associated with the energy exchange between the optical and mechanical modes lead to a wide diversity of dynamics of such resonators [1], e. g., to self−oscillations with frequency $F$ close to the eigen frequency $f$ of the OMO elastic oscillations. Along with this, the optical radiation interaction with several microoscillators simultaneously induces a number of new interesting phenomena [2] enabling expansion of the application area of such systems. In recent years, a reasonable continuation of these studies, namely, laser optomechanics connected with investigating the interaction between the laser radiation and OMO in active (laser) resonators was significantly developed [3–5]. Taking into account the laser dynamics specific features, it is possible to implement in them different−type internal resonances essentially defining the laser radiation generation modes and characteristics. In this connection, especially interesting are fiber lasers (FL) possessing, along with unique specific features, a great variety of dynamic modes [6]. In the FL−OMO laser systems [5], for instance, under the resonance conditions ($f \approx f_{rel}$ is the FL relaxation oscillations frequency), synchronous self−oscillations (SO) are possible; they provide modulation of the amplitude, frequency, and polarization of the generated radiation with the OMO elastic oscillation frequency $F = (1+\alpha)f$, $\alpha \ll 1$. In view of the elastic oscillation modes dependence on external impacts upon OMO, this opens opportunities for creating FL with a controllable combined modulation of the radiation parameters, as well as self−generation fiber−optic sensors with a wide dynamic range and high measurement accuracy [1,7,8].

An important feature of the self−oscillation systems with many degrees of freedom is the possibility of realizing in them multifrequency SO providing reduction of the self−oscillation frequency fluctuations [9], which allows extension of functional capabilities and improvement of the accuracy of devices based on such systems. Notice that, to our knowledge, there are no studies devoted to multifrequency SO in lasers with OMO, except for work [10] where the modes of double−frequency self−oscillations were for the first time realized in a fiber laser with microoscillators. This confirms the topicality of this work which is, to a high extent, an evolution of [10]. In view of the scientific and practical importance of erbium−ytterbium FL [6], the studies in this work were performed using the mentioned FL and multifrequency OMO fabricated in the form of a multicomponent planar silicon structure used as a mirror ($M$) in the laser resonator (Fig. 1).

In the FL−OMO laser system under consideration, the generated radiation ($\lambda_s \approx 1.54\,\mu$m) interacts simultaneously with several microoscillators fabricated in the form of elastic−oscillation elements, namely, silicon microbeams with bilateral rigid fixation on supports ($MB_i$, $i = 1-13$), which form an axially symmetric array. $MB_i$ have equal thicknesses $h \approx 6\,\mu$m but different lengths and widths ($l_i$, $b_i$). Laser excitation of transverse waves in $MB_i$ formed on the common epitaxial plate using anisotropic etching occurs under the light−pressure force (contrary to the photothermal effect in [10]) due to the high reflection factor ($R_s \approx 0.9$) of the multilayer ($SiO_2 + ZrO_2$) interference film applied on the $MB_i$ surfaces. The OMO reflective surface is located in the focal plane of the autocollimation system with a cylindrical lens forming a linear light spot (LLS) ($D$; $d$) $\approx$ (380; 12 $\mu$m) in size, which can intersect up to five microbeams interacting with the laser radiation (depending on the orientation angle $\varphi$ and distance $l_0$ to its center). The required mutual

orientation of the laser beam and OMO was ensured with a micropositioner. Relatively large inter−$MB_i$ distance $\big(h \ll (z; H) \approx (60; 200\,\mu\text{m})\big)$ allows neglecting during oscillations the $MB_i$ mutual influence via visco−elastic perturbations in the vicinity of the supports and in the environment. In view of stiffening of the synchronization conditions with increasing dispersion of beat frequencies and number of oscillators [9], notice especially the OMO spectrum quasiequidistant character, namely, proximity of differences $(\Delta_n)$ between eigen frequencies $(f_{n,i})$ for the $n$-th mode of the neighboring $MB_i$ transverse oscillations: $\Delta_n = f_{n,i+1} - f_{n,i}$, $\Delta_n \ll f_{n,i}$. This is realized by varying the $MB_i$ lengths: I. $l_i = 4\big(1 + 0.002(i-1)\big)$ mm, $i = 1{-}7$; II. $l_i = 4\big(1 + 0.014(i-7)\big)$ mm, $i = 8{-}13$. For the specified $MB_i$ groups with $n = 5$, 6, estimates of the following quantities were experimentally obtained: I. $(\Delta_5^{\text{I}}; \Delta_6^{\text{I}}) \approx (0.3{-}0.5; 0.6{-}0.8)$ kHz; II. $(\Delta_5^{\text{II}}; \Delta_6^{\text{II}}) \approx (2.4{-}3; 3.5{-}4)$ kHz; eigen frequencies of the $MB_i$ modes are $(f_{5,i}; f_{6,i}) \approx (65{-}78; 96{-}118)$ kHz, their mechanical Q−factors are $Q_{5,i}$; $Q_{6,i} \geqslant 300$ (in air). The broad range of $MB_i$ widths $(b_1; b_{13}) = (20; 210\,\mu\text{m})$ taking into account conditions $\Delta_5^{\text{I}}$, $\Delta_5^{\text{II}} \geqslant f_{5,i}/Q_{5,i}$, $\Delta_6^{\text{I}}$, $\Delta_6^{\text{II}} \geqslant f_{6,i}/Q_{6,i}$ excluding overlapping of resonance lines of these modes allows selecting different sets of different−frequency $MB_i$ interacting with laser radiation.

Notice a number of the FL−OMO specific features.

1. The $MB_i$ oscillations were determined by Fourier analysis of the $M$ effective reflection factor $R_{eff}(t) = V_3(t)/V_2(t)$ that was measured by using a fiber splitter with short output lengths $S_{1,2,3} \ll c f^{-1}$ under the conditions of complex dynamics of radiation falling on OMO, $P_s(t) \propto V_2(t)$.

2. As an active medium, there was used an erbium−ytterbium active fiber (AF) with pump into the multimode shell [6], which prevents the pump radiation $(\lambda_p \approx 976\,\text{nm})$ propagation in the FL optical resonator.

3. As the mirror $M_0$, both the broadband reflectors (BBR, $\Delta\lambda_1 \approx 80\,\text{nm}$) in the form of interference films at the fiber ends with reflection factors $R_s = 0.5{-}0.9$ and narrowband $(\Delta\lambda_2 \approx 0.6\,\text{nm})$ fiber Bragg gratings with $R(\lambda_s) = 0.6{-}0.95$ (FBG) were used.

The mean power of the laser radiation falling on OMO could be varied within the $\bar{P}_s = 0{-}25\,\text{mW}$ range by controlling power $P_p$ of the continuous pump radiation; in view of variations in the FL fiber−optic resonator length $L$ (free of considerable loss variations), this allows also controlling frequency $f_{rel}(P_p, L)$. The results presented below were obtained under different resonance conditions: $f_{rel} \approx f_{5,i}$, i. e. $f_{rel}$ in the resonance with the $MB_i$ 5-th harmonic or $f_{rel} \approx f_{6,i}$; in this case, we restrict ourselves to the data obtained at $\varphi = 90^\circ$ (LLS is orthogonal to $MB_i$). To efficiently excite OMO oscillations providing the $R_{eff}$ modulation, LLS was arranged either along the OMO symmetry axis passing through the odd−mode central nodes or on even−mode nodes nearest to this axis and closest to each other. Since $R_{eff}$ is defined by the interference of waves reflected from all the irradiated $MB_i$, the dependence of phase incursions of these waves on angle $\theta$ between the laser beam axis and normal to the OMO surface causes the complexity of the $R_{eff}(\theta)$ shape and multifrequency SO excitation zones in the form of $(\theta_1, \theta_2)$ regions within the beam diffraction divergence $\sim \lambda_s / b_{\max} \leqslant 3 \cdot 10^{-2}$ rad, where $b_{\max} = \max\{b_i - b_k\}$.

Fig. 1 demonstrates the oscillograms and Fourier spectrum of signal $V_2(t) \propto P_s(t)$ in the mode of double−frequency self−oscillations $\big(\text{SO}(2)\big)$ in the system with a broadband mirror $(R_s \approx 0.8)$ where the laser radiation interacts with two $MB_i$: $(b_9; b_{10}) = (90; 115\,\mu\text{m})$, $\Delta_5^{\text{II}} \approx 3\,\text{kHz}$ at $f_{rel} \approx (f_{5,9}; f_{5,10}) \approx (72; 69\,\text{kHz})$. SO(2) arise at $P_p > P_{th}(2)$ that is a threshold value related with $\bar{P}_s \approx 12\,\text{mW}$. The $P_s(t)$ comb spectrum frequency range is $\Delta\nu \approx \Delta_5^{\text{II}}$. Noteworthy is that the $P_s(t)$ envelope is qualitatively similar to the envelope presented in [10]. Similar SO(2) comb spectra are observed also at the $f_{rel} \approx f_{6,i}$ resonance with $\Delta\nu \approx \Delta_6^{\text{I}}(\Delta_6^{\text{II}})$. Notice that at $f_{rel} \approx f_{5,i}(f_{6,i})$ SO(2) may take place also in case LLS intersects more than two microbeams.

Three—, four— and five-frequency modes $\big(\text{SO}(3){-}\text{SO}(5)\big)$ were obtained using the group I microbeams and broadband reflectors as $M_0$. Fig. 2, *a*, *b* presents the $P_s(t)$ envelope and spectrum corresponding to SO(3) at

$$f_{rel} \approx (f_{6,5}; f_{6,6}; f_{6,7}) \approx (104.7; 104; 103.2\,\text{kHz}),$$

when the radiation interacts with three $MB_i$: $(b_5; b_6; b_7) = (40; 50; 60\,\mu\text{m})$. The $P_s(t)$ envelope with the expected period $T(3) \approx (\Delta_6^{\text{I}})^{-1} \approx 1.2\,\text{ms}$ has a complex structure with one sidelobe between two main peaks; the quasicontinuous $P_s(t)$ spectrum contains several lines close to $f_{6,5}; f_{6,6}; f_{6,7}$ which are better pronounced at high spectral resolution. Excitation of SO(3) occurs in a soft mode at $P_p > P_{th}(3) > P_{th}(2)$, where threshold $P_{th}(3)$ is quite sensitive not only to the transverse LLS shifts but also to longitudinal ones, which is probably caused by inhomogeneity of the lineal radiation power along LLS. The $P_s(t)$ envelope and spectrum shown in Fig. 3, *a* correspond to SO(4) arising in the laser radiation interaction with four $MB_i$ $(b_5; b_6; b_7; b_8) = (40; 50; 60; 70\,\mu\text{m})$ at $f_{rel} \approx f_{5,i}$. In this case, there are two sidelobes within the envelope period $T(4) \approx (\Delta_5^{\text{I}})^{-1} \approx 2.7\,\text{ms}$. The $P_s(t)$ spectrum has a maximum at $\nu_{\max} \approx f_{5,6} \approx 75\,\text{kHz}$ (the Fig. 3, *a* inset) and is almost fully continuous; its width is several times larger than the $(f_{5,5}; f_{5,8})$ interval, which is probably connected with generation in this nonlinear system of combination frequencies $f_{5,6} \pm k\Delta_5^{\text{I}}$, $k = 1, 2, \ldots$ . Fig. 3, *b* demonstrates the $P_s(t)$ envelope obtained in the SO(5) mode at $f_{rel} \approx f_{5,i}$. In this case, the spectrum is also continuous. Here there are three sidelobes (pulses) within the envelope period $T(5) \approx (\Delta_5^{\text{I}})^{-1} \approx 4\,\text{ms}$. Noteworthy is high sensitivity of SO(4) and, especially, of SO(5), to perturbations of the system, for instance, of parameters $(l_0, \theta)$, which results in SO quenching and unstable „spike“

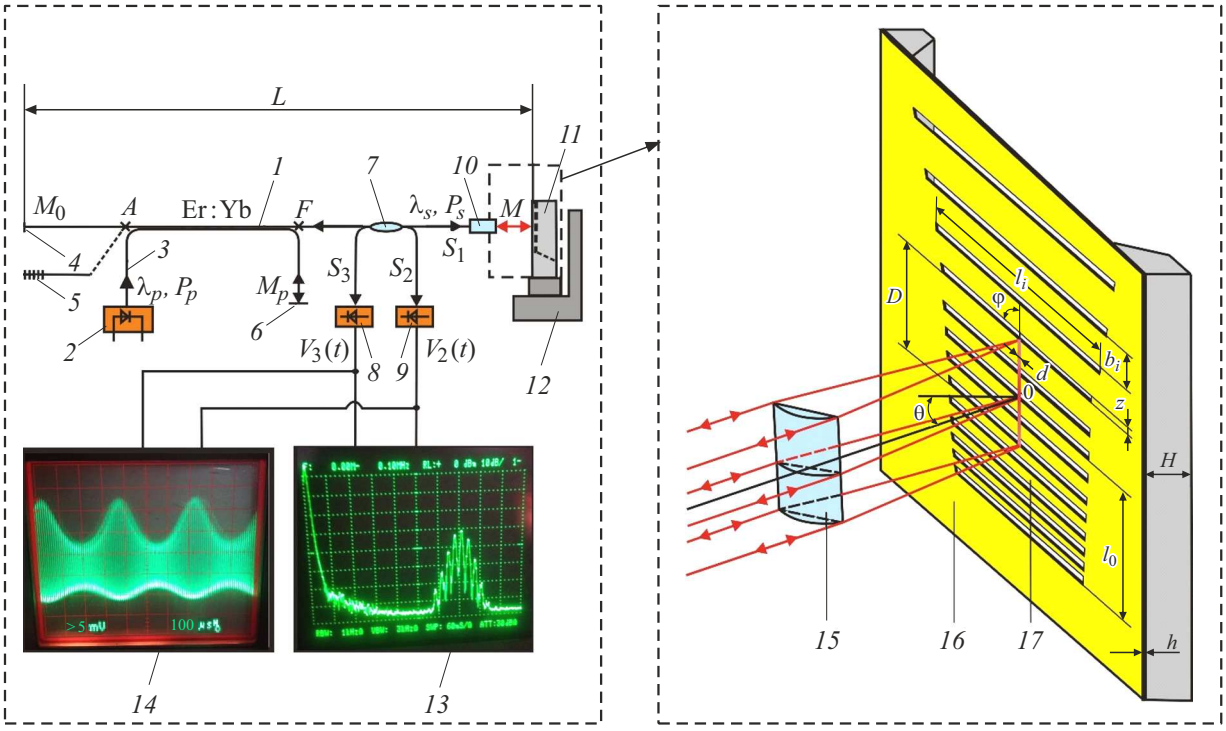


**Figure 1.** The FL–OMO laser system layout. *1* — erbium–ytterbium active fiber; $l_{AF} \approx 3$ m; *2* — pumping laser diode with a multimode fiber output *3*; *4* — stationary mirror ($M_0$); *5* — Bragg grating (FBG); *6* — pumping radiation reflector ($M_p$); *7* — single–mode fiber splitter (90 : 10); *8*, *9* — photoreceivers (InGaAs); *10* — collimator; *11* — OMO (mirror $M$); *12* — micropositioner; *13* — radiofrequency spectrum analyzer; *14* — oscilloscope; *15* — cylindrical lens; *16* — silicon epitaxial plate with OMO; *17* — microbeam ($i = 4$).

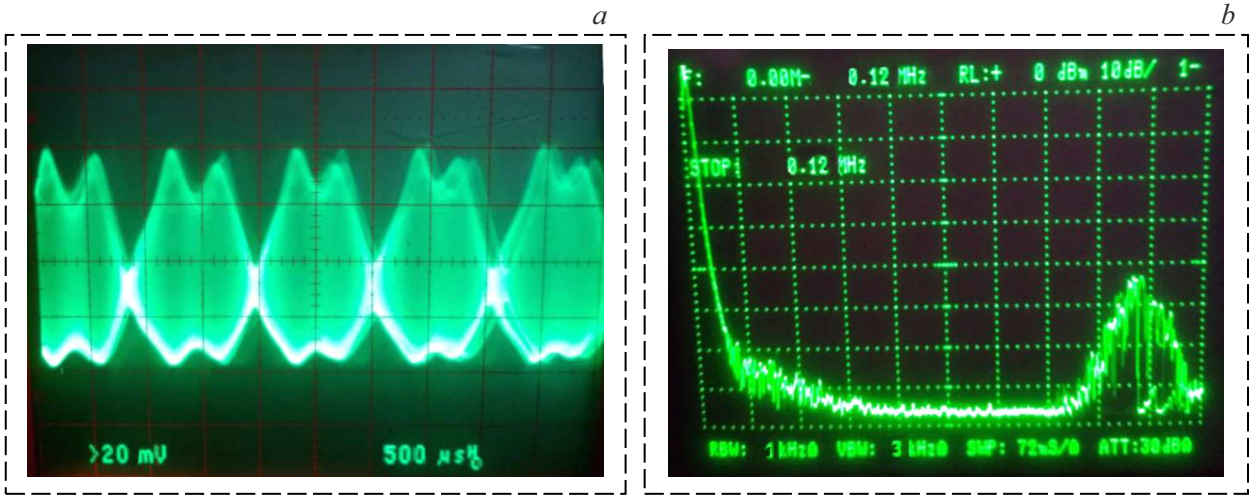


**Figure 2.** Envelope oscillogram ($a$) and Fourier spectrum ($b$) of the laser radiation power $P_s(t)$ in the SO(3) mode at $f_{rel} \approx (f_{6,5};\ f_{6,6};\ f_{6,7}) \approx (104.7;\ 104;\ 103.2\,\text{kHz})$; MB$_i$: $(b_5;\ b_6;\ b_7) = (40;\ 50;\ 60\,\mu\text{m})$.

modes with the $P_s(t)$ envelope in the form of random groups of pulses with different amplitudes and lengths. This is probably caused by an error in the OMO modes synchronization due to the random phase „failures“ .

Experiments in which BBR or FBG were used as mirror $M_0$ have established that at $f_{rel} \approx f_{5,i}(f_{6,i})$: 1) in the systems with FBG even with high reflection factor $R(\lambda_s) = 0.95$ in case of the $P_p$ variations within the operating range, only SO(2) with low signal/noise ratio were excited, while in the case of BBR with the minimal reflection factor $R_s = 0.5$, SO(3) and SO(4) were also excited; 2) in the case of equal BBR and FBG reflection factors, the SO(2) excitation threshold in the system with FBG is 30–40% higher than with BBR. These features may be explained by the effect of AF inhomogeneous broadening. As known [11], the uniform amplification

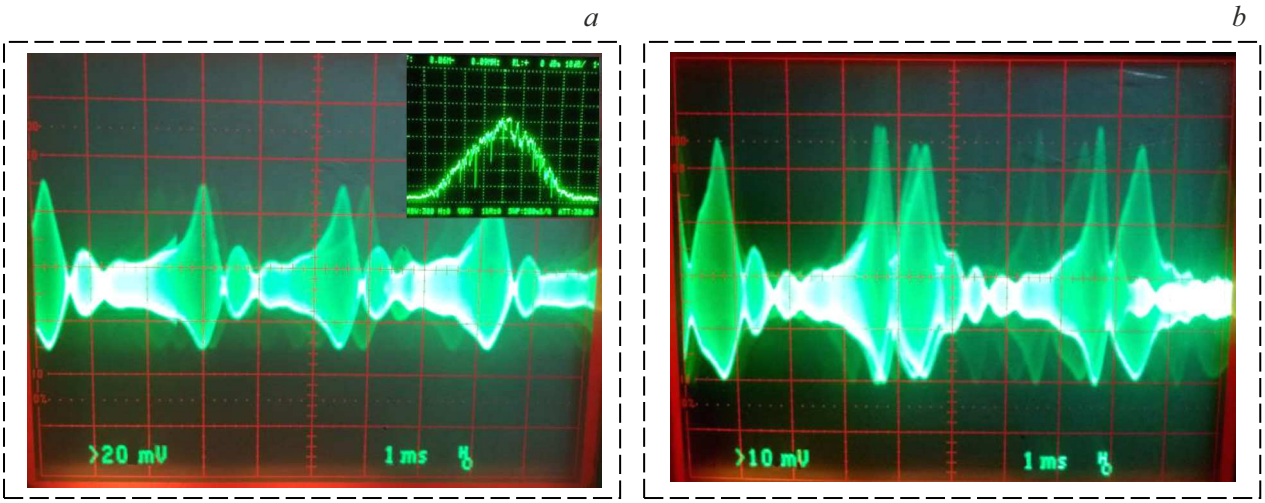


**Figure 3.** *a* — $P_s(t)$ envelope oscillogram in the SO(4) mode (in the inset: $P_s(t)$ spectrum in the range of 60−90 kHz); *b* — $P_s(t)$ envelope oscillogram in the SO(5) mode at $f_{rel} \approx f_{5,i}$.

spectrum width in erbium AF is $\Delta\lambda_h \ll \Delta\lambda_{ase}$, where $\Delta\lambda_{ase}$ is the superluminescence (amplification) spectrum width, while in AF it is $(\Delta\lambda_h; \Delta\lambda_{ase}) \approx (0.5; 20\,\text{nm})$; therefore in the systems with FBG $\Delta\lambda_2 \approx 0.6\,\text{nm}$ in width, the OMO oscillations give rise to modulation of only a small part of the laser resonator radiation spectrum, $\sim (\Delta\lambda_h^2 + Delta\lambda_2)^{1/2}/\Delta\lambda_{ase} \ll 1$, which may explain the low FBG efficiency in exciting SO in the laser systems under consideration.

Thus, in fiber lasers with optomechanical microoscillators there were realized for the first time multifrequency (up to five frequencies) synchronous self−oscillations providing unique modulation characteristics of the generated laser radiation.

### Financial support

The study was accomplished in the framework of State Assignment for Kotelnikov IRE of RAS.

### Conflict of interests

The author declares that he has no conflict of interests.

## References

[1] B.B. Li, L. Ou, Y. Lei, Y.C. Liu, Nanophotonics, **10** (11), 27 (2021). DOI: 10.1515/nanoph-2021-0256
[2] M.F. Colombano, G. Arregui, N.E. Capuj, A. Pitanti, J. Maire, A. Griol, B. Garrido, A. Martinez, C.M. Sotomayor-Torres, D. Navarro-Urrios, Phys. Rev. Lett., **123** (1), 017402 (2019). DOI: 10.1103/PhysRevLett.123.017402
[3] D. Princepe, G.S. Wiederhecker, I. Favero, N.C. Frateschi, IEEE Photon. J., **10** (3), 4500610 (2018). DOI: 10.1109/JPHOT.2018.2831001
[4] X. Xi, J. Ma, X. Sun, Phys. Rev. A, **99** (5), 05383 (2019). DOI: 10.1103/PhysRevA.99.053837
[5] F.A. Egorov, V.T. Potapov, Quantum Electron., **50** (8), 734 (2020). DOI: 10.1070/QEL17116.
[6] V.V. Ter-Mikirtychev, *Fundamentals of fiber lasers and fiber amplifiers*, 2nd ed. (Springer, 2019). DOI: 10.1007/978-3-319-02338-0-9
[7] E. Buks, I. Martin, Phys. Rev. E, **100** (3), 032202 (2019). DOI: 10.1103/PhysRevE.100.032202
[8] F.A. Egorov, V.T. Potapov, Foton-ekspress, № 7, 3 (2018). http://fotonexpres.ru/bez-rubriki/vyshel-iz-pechati-foton-ekspress-7 (in Russian)
[9] P.S. Landa, *Nelineynye kolebaniya i volny*, 2-e izd. (LIBROKOM, M., 2010). (in Russian)
[10] V.D. Burkov, F.A. Egorov, V.T. Potapov, Tech. Phys., **50** (1), 69 (2005). DOI: 10.1134/1.1854826.
[11] S.K. Morshnev, N.I. Starostin, Ya.V. Przhiyalkovsky, A.I. Sazonov, Quantum Electron., **50** (10), 904 (2020). DOI: 10.1070/QEL17347.